Transport and Communications Science Journal

UNSUPERVISED LEARNING FOR STRUCTURAL HEALTH MONITORING: A MULTI-STATION GNSS-RTK APPROACH FOR OPERATIONAL STATE DETECTION IN CABLE-STAYED BRIDGES

Tran Duc Cong, Le Khanh Giang*, Ho Thi Lan Huong

University of Transport and Communications, No 3 Cau Giay Street, Hanoi, Vietnam

ARTICLE INFO

TYPE: Research Article
Received: 04/04/2026
Revised: 05/11/2026
Accepted: 11/11/2026
Published online: 15/11/2026
https://doi.org/10.47869/tcsj.77.9.10

* *Corresponding author*
Email: gianglk@utc.edu.vn; Tel: +84983663031

Abstract. Monitoring the operational condition of cable-stayed bridges is essential for ensuring structural safety and long-term serviceability. GNSS-RTK technology has emerged as an effective solution for continuous, high-precision displacement measurement in structural health monitoring (SHM). However, high-frequency GNSS data are often noisy and unlabeled, posing significant challenges for traditional analysis methods. This study addresses the problem of identifying structural operational states from unlabeled GNSS-RTK data using an unsupervised learning framework. Displacement data collected from two GNSS stations installed symmetrically on a cable-stayed bridge were segmented into hourly windows and preprocessed using Hampel filtering and Kalman smoothing. Feature vectors were then standardized and reduced in dimensionality using Principal Component Analysis, while t-SNE was applied for visualization. Clustering algorithms, including K-Means, hierarchical agglomerative clustering, Gaussian mixture models, and DBSCAN, were implemented and evaluated using multiple internal validation indices and stability metrics. The results reveal a consistent two-state structure in the horizontal displacement component, with K-Means achieving the best performance (Silhouette score up to 0.7006) and perfect stability (ARI = 1.0). Importantly, the clustering results are highly consistent across both stations, indicating strong spatial reliability. These findings demonstrate that unsupervised learning can effectively extract meaningful operational states from GNSS-RTK data, providing a robust and scalable approach for structural health monitoring of large-scale bridges.

Keywords: cable-stayed bridge, GNSS-RTK, structural health monitoring, unsupervised learning, clustering, operational state detection.

@ 2026 University of Transport and Communications

1. INTRODUCTION

Cable-stayed bridges are among the most advanced long-span structural systems, characterized by high slenderness and sensitivity to operational loads and environmental factors such as wind, temperature, and traffic. Therefore, continuous monitoring of their structural performance through Structural Health Monitoring (SHM) systems plays a crucial role in ensuring operational safety and extending service life. Among existing monitoring technologies, the Global Navigation Satellite System Real-Time Kinematic (GNSS-RTK) has been proven to be an effective solution for measuring absolute displacements of large-scale structures with high accuracy in real time [1,2]. With its capability to provide continuous and stable three-dimensional displacement measurements, GNSS-RTK is particularly suitable for monitoring cable-stayed bridges and other large infrastructures.

However, GNSS-RTK data in practice exhibit several complexities, including non-stationarity caused by environmental and operational conditions, signal loss, structured noise such as atmospheric errors and multipath effects, and the lack of labeled information regarding structural states [2,3]. These characteristics limit the effectiveness of traditional statistical and physics-based analysis methods, particularly in the context of large-scale and highly dynamic datasets.

In recent years, machine learning (ML) has emerged as a promising approach in SHM, especially unsupervised learning (UL) methods for handling unlabeled data. Study [4] suggests that SHM can be formulated as a statistical pattern recognition problem, where UL plays a key role in detecting changes in system states. In this context, clustering techniques provide an effective tool for uncovering latent structures in data and distinguishing different operational states of structures.

Previous studies have explored UL for GNSS-based SHM. For instance, the study [5] proposed a framework combining t-SNE and K-Means clustering to identify latent patterns, while the research [6] applied clustering methods such as Hierarchical Agglomerative Clustering (HAC) and Gaussian Mixture Models (GMM) to vertical GNSS-RTK data of cable-stayed bridges. However, these studies primarily focus on single-station data and do not comprehensively evaluate clustering stability or spatial consistency across monitoring locations.

Despite these efforts, several limitations remain in existing studies: (i) reliance on a single clustering algorithm or limited comparisons; (ii) use of simulated or single-station data; (iii) insufficient evaluation of clustering stability and parameter sensitivity; and (iv) lack of validation under real-world multi-station monitoring conditions [5,6]. Therefore, an important research question arises: can UL algorithms reliably and consistently identify structural operational states from unlabeled multi-station GNSS-RTK data under real-world conditions?

To address this question, this study proposes an integrated UL framework for detecting operational states of cable-stayed bridges using GNSS-RTK data. The framework is validated using real-world data collected from two GNSS stations (4E and 4W) installed symmetrically on the same cross-section of Nhat Tan Bridge, enabling the assessment of spatial consistency in the detected states.

Specifically, the objectives of this study are to: (i) develop an integrated processing pipeline combining signal processing and ML for GNSS-RTK data; (ii) compare the performance of representative clustering algorithms (K-Means, HAC, GMM, and Density-Based Spatial

Clustering of Applications with Noise (DBSCAN)); (iii) evaluate clustering quality and stability using internal validation indices and Adjusted Rand Index (ARI); and (iv) analyze spatial consistency between the two GNSS stations to verify the physical significance of the detected operational states.

The main contributions of this study are threefold: (i) proposing a comprehensive GNSS-RTK data analysis framework for SHM applications; (ii) providing a systematic and quantitative comparison of clustering algorithms using real-world data; and (iii) demonstrating the ability to detect operational states with strong spatial consistency across multiple monitoring stations, thereby enhancing the reliability of SHM systems.

2. STUDY DATA AND METHODS

2.1. Study data

In this study, GNSS-RTK displacement time series collected from the mid-span girder of Nhat Tan Bridge are analyzed. Specifically, the data were obtained from two monitoring points, denoted as 4W and 4E (Figure 1), located on the main beam corresponding to the upstream and downstream sides. These points are part of the bridge monitoring system and record displacement data at a sampling frequency of 1 Hz, including three components: longitudinal displacement (X), transverse displacement (Y), and vertical displacement (h). The GNSS-RTK time series at stations 4W and 4E were continuously collected over a period of 14 days, from May 29 to June 11. This duration is sufficiently long to capture a variety of operational and environmental conditions affecting the bridge.

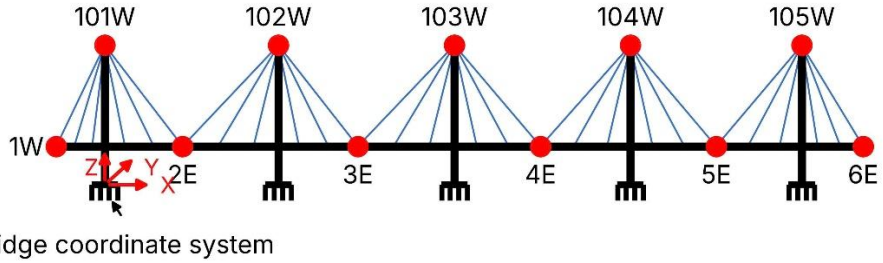


Figure 1. Locations of GNSS stations 4E and 4W on the cross-section of Nhat Tan Bridge [7].

Although the GNSS-RTK system provides three-dimensional displacement measurements (X, Y, h), preliminary analysis reveals significant differences in signal quality among the components. In particular, the vertical displacement (h_Coord) exhibits a high level of noise, including large-amplitude outliers, especially at station 4E. In contrast, the horizontal components (X and Y) demonstrate greater stability and more clearly reflect the dynamic behavior of the structure. Among these, the longitudinal component (X_Coord) shows the most distinct and consistent clustering patterns across both stations and achieves the highest stability according to the ARI in clustering experiments. Therefore, in this study, the analysis focuses on the X component as a representative indicator of structural behavior. Although the vertical displacement (h) is an important indicator of bridge dynamic behavior at the mid-span, all displacement components were evaluated during the preliminary analysis. The X component was selected for detailed investigation because it demonstrated the most stable and consistent clustering performance across both monitoring stations. This choice not only improves the signal-to-noise ratio but also enhances the interpretability and effectiveness of the UL algorithms. Based on this dataset, an integrated analysis framework is developed to identify operational states of the bridge, as described in the following section.

2.2. Methodology

This study proposes an integrated methodological framework for detecting operational states of cable-stayed bridges from GNSS-RTK data using UL. The objective of the proposed pipeline is to exploit latent structures in monitoring data to identify different structural operating states without requiring labeled information.

The overall analysis workflow is illustrated in Figure 2 and consists of the following main steps: (i) preprocessing of GNSS data to remove noise and outliers; (ii) segmentation and feature extraction based on time windows; (iii) data normalization and dimensionality reduction; (iv) clustering using UL algorithms (K-Means, HAC, GMM, and DBSCAN); and (v) evaluation of clustering quality and stability.

The workflow is applied independently to each GNSS station (4E and 4W), followed by a comparison of the results to assess the spatial consistency of the detected operational states. This approach enables the distinction between actual structural dynamic behavior and local variations caused by sensor-specific effects.

2.2.1. Data preprocessing

GNSS-RTK data in real-world applications are often affected by various types of noise and measurement errors, including multipath effects, atmospheric disturbances, and occasional signal interruptions [3]. Therefore, data preprocessing is a critical step to ensure the reliability and quality of the input data for subsequent analysis.

First, the continuous GNSS time series are segmented into fixed-length time windows of one hour (corresponding to 3600 samples at a sampling rate of 1 Hz). Time windows with more than 5% missing data are discarded to ensure data completeness. To maintain consistency in multi-station analysis, only time windows with valid data at both stations (4E and 4W) are retained for further processing.

Next, the Hampel filter is applied to detect and remove outliers in the time series [6]. This method

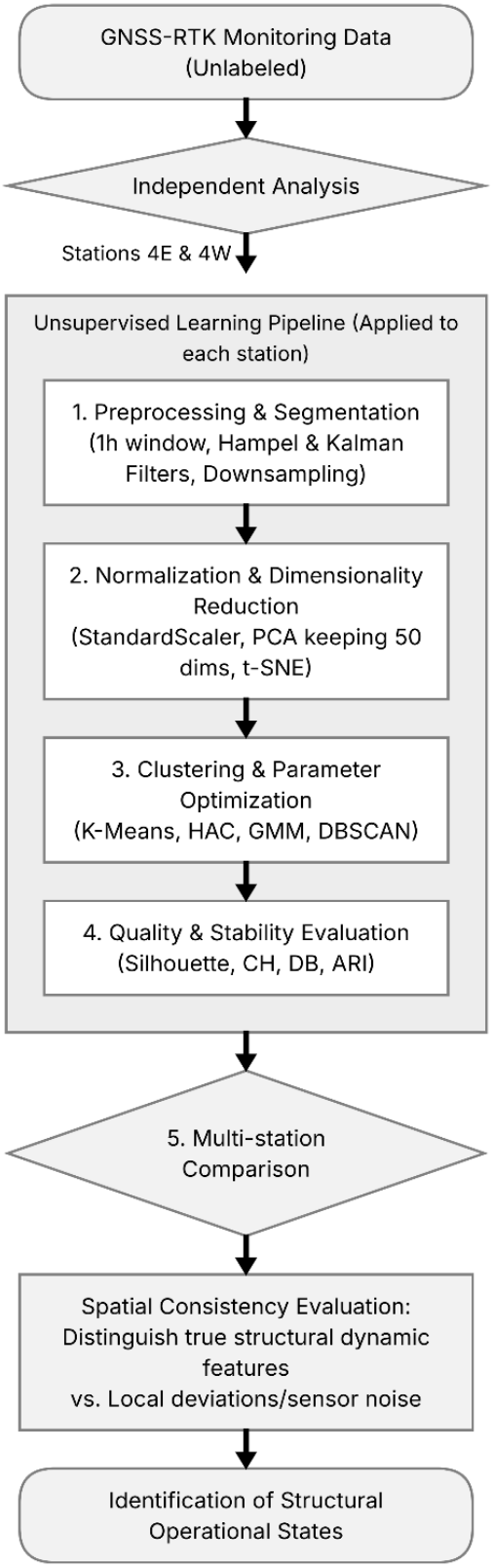


Figure 2. Proposed workflow for GNSS-RTK data processing and analysis.

utilizes a sliding window approach based on the local median and the median absolute deviation (MAD) to identify abnormal values. It is particularly effective in eliminating impulsive noise commonly observed in GNSS measurements.

After outlier removal, a Kalman filter is employed to smooth the time series and reduce residual random noise [2]. The Kalman filter is implemented as a linear state-space model, providing optimal estimates of the true system state based on noisy observations. Finally, each time window is transformed into a fixed-length feature vector through downsampling, reducing the number of samples from 3600 to 360 points. This step decreases data dimensionality while preserving the essential dynamic characteristics of the signal.

Overall, the preprocessing procedure enhances data quality, suppresses noise, and highlights meaningful structural responses, thereby improving the effectiveness of subsequent UL algorithms.

2.2.2. Data normalization and dimensionality reduction

Before clustering, the extracted feature vectors are standardized to ensure that all variables contribute equally to the analysis. Standardization is performed using the StandardScaler method, which transforms each feature to have zero mean and unit variance [8]. Although all GNSS displacement components share the same unit (meters), differences in variance and magnitude may bias distance-based clustering algorithms such as K-Means and HAC. Therefore, this step is essential to achieve a balanced representation of the data in the feature space.

Following normalization, Principal Component Analysis (PCA) is applied to reduce data dimensionality and remove redundant information [9]. PCA performs a linear transformation that projects the original feature space onto a set of orthogonal components, ranked according to their explained variance. This transformation helps to mitigate noise, reduce feature correlation, and improve the structure of the data for clustering.

In this study, the number of principal components is set to 50, which preserves nearly all the variance in the original data (explained variance $\approx$ 100%). This indicates that the selected components are sufficient to retain the essential information while significantly reducing data dimensionality. The combination of standardization and PCA not only improves computational efficiency but also enhances the separability of clusters in the feature space. As a result, subsequent clustering algorithms can operate more effectively and produce more stable and reliable results.

2.2.3. Data visualization using t-SNE

To support the interpretation of the data structure after preprocessing and dimensionality reduction, t-Distributed Stochastic Neighbor Embedding (t-SNE) is employed to visualize the high-dimensional feature space in two dimensions. t-SNE is a nonlinear dimensionality reduction technique that preserves local neighborhood relationships by modeling pairwise similarities between data points in both the original and embedded spaces [10]. As a result, it is particularly effective for revealing latent cluster structures in complex datasets.

In this study, t-SNE is used solely for visualization purposes to qualitatively assess the separability of the data after preprocessing and PCA. The clustering analysis is conducted in the PCA-transformed feature space rather than in the t-SNE space, to avoid distortions introduced by nonlinear embedding.

It should be noted that t-SNE does not preserve global distances, and the relative positions between clusters in the two-dimensional space may not accurately reflect their relationships in

the original high-dimensional space. Therefore, the t-SNE representation is used only as a visual aid, while the evaluation of clustering performance is based on quantitative metrics computed in the original feature space. By providing an intuitive visualization of the data distribution, t-SNE facilitates the qualitative interpretation of clustering results and supports the identification of underlying structural patterns in GNSS-RTK data.

2.2.4. Clustering algorithms

To comprehensively evaluate the ability to identify latent operational states from GNSS-RTK data, four representative clustering algorithms are employed in this study, including K-Means, HAC, GMM, and DBSCAN. These algorithms are selected to cover different clustering paradigms, including distance-based, hierarchical, probabilistic, and density-based approaches. All clustering methods are applied to the feature space obtained after PCA transformation to ensure consistency and to reduce the influence of noise and feature correlation.

K-Means is a partition-based clustering algorithm that assigns data points to clusters by minimizing the within-cluster variance. It assumes that clusters are compact and approximately spherical in shape, making it suitable for detecting well-separated structures in the data.

HAC is a bottom-up clustering method that iteratively merges data points or clusters based on a linkage criterion. In this study, Ward's method is adopted to minimize the total within-cluster variance, allowing the identification of hierarchical relationships in the data without requiring an initial specification of cluster centroids.

GMM represent a probabilistic approach to clustering, where the data are modeled as a mixture of Gaussian distributions. Unlike K-Means, GMM can capture clusters with elliptical shapes and varying covariance structures, providing greater flexibility in modeling complex data distributions.

DBSCAN is a density-based clustering algorithm that groups data points based on local density and identifies outliers as noise. This method is particularly suitable for datasets containing irregular cluster shapes and noise, which are common characteristics of GNSS-RTK measurements.

The use of multiple clustering algorithms with different underlying assumptions enables a comprehensive analysis of the GNSS-RTK data. By comparing their performance, the study aims to identify the most suitable method for detecting operational states while also assessing the robustness and consistency of the clustering structure. This multi-algorithm approach provides deeper insight into the intrinsic structure of the data and reduces the risk of bias associated with relying on a single clustering technique.

2.2.5. Parameter selection

Appropriate selection of clustering parameters is critical to ensure the reliability and interpretability of the results. In this study, parameter tuning is conducted systematically for each clustering algorithm based on quantitative criteria, rather than subjective assumptions.

For algorithms that require a predefined number of clusters (K-Means, HAC, and GMM), the optimal number of clusters k is determined through a parameter sweep in the range of 2 to 10. The Silhouette coefficient is adopted as the primary criterion, as it evaluates both intra-cluster cohesion and inter-cluster separation [11]. The optimal value of k is selected at the point where the Silhouette score reaches its maximum, while also considering the overall trend to avoid over-segmentation.

For the GMM approach, in addition to determining the number of components, different covariance structures (e.g., full, diagonal, tied, spherical) are evaluated. The optimal model configuration is selected using the Bayesian Information Criterion (BIC), which balances model fit and complexity [12].

For DBSCAN, the two key parameters, namely the neighborhood radius (ε) and the minimum number of points (MinPts), are determined based on the k-distance graph. The value of ε is selected at the "elbow" point of the curve, representing a transition between dense and sparse regions [13]. The value of MinPts is chosen considering the dimensionality of the feature space after PCA, ensuring that the density criterion is consistent with the data structure.

To improve the robustness of cluster selection, a voting-based strategy is adopted to determine the optimal number of clusters. Specifically, candidate values of k obtained from different clustering algorithms (K-Means, HAC, and GMM) are aggregated for each coordinate component and each GNSS station. The final value of k is then selected based on majority agreement across algorithms, while also considering consistency between the two GNSS stations. This strategy reduces the bias associated with any single algorithm and ensures that the selected clustering configuration reflects both algorithmic consensus and spatial consistency.

The results of this voting-based selection are presented in Section 3.3. Overall, this systematic parameter selection strategy ensures that the clustering results are data-driven and reproducible. Moreover, consistency in the selected parameters across the two GNSS stations is further examined as an additional indicator of robustness and spatial reliability.

2.2.6. Evaluation metrics

Since GNSS-RTK data used in this study are unlabeled, the performance of clustering algorithms is evaluated using internal validation metrics. To ensure a comprehensive assessment, multiple complementary indices are employed, including the Silhouette Coefficient, Calinski–Harabasz Index, and Davies–Bouldin Index.

The Silhouette Coefficient measures the degree of similarity of a data point to its own cluster compared to other clusters, providing an overall indication of cluster cohesion and separation. Higher values indicate better-defined and more distinct clusters [11]. The Calinski–Harabasz Index evaluates the ratio of between-cluster variance to within-cluster variance, reflecting the overall separability of clusters in the feature space [14]. In contrast, the Davies–Bouldin Index measures the average similarity between clusters, where lower values indicate better clustering performance with more compact and well-separated clusters [15].

In addition to clustering quality, the stability of the results is assessed using the ARI [16]. The ARI quantifies the similarity between clustering results obtained from multiple runs with different initializations. A value of ARI close to 1 indicates highly consistent and stable clustering outcomes, while lower values suggest sensitivity to initialization or parameter settings.

The combined use of multiple internal metrics and stability analysis provides a robust evaluation framework for clustering performance. This is particularly important in structural health monitoring applications, where reliable and consistent results are essential for long-term monitoring and decision-making. Furthermore, the consistency of evaluation metrics across the two GNSS stations is analyzed as an additional indicator of spatial reliability. Consistent performance between stations supports the interpretation that the detected clusters correspond to actual structural operational states rather than sensor-specific artifacts.

2.2.7. Multi-station analysis

Multi-station analysis plays a crucial role in this study by enabling the assessment of spatial consistency in the detected operational states. The two GNSS stations (4E and 4W) are symmetrically installed on the same cross-section of the bridge, providing an ideal configuration to validate whether the identified clustering patterns reflect true structural behavior rather than sensor-specific artifacts.

The complete analysis pipeline, including preprocessing, dimensionality reduction, clustering, and evaluation, is applied independently to each station. This independent processing ensures that the results are not influenced by shared preprocessing assumptions or data fusion effects.

Subsequently, the clustering results obtained from the two stations are systematically compared based on several criteria, including the optimal number of clusters, clustering performance metrics (Silhouette, Calinski–Harabasz, and Davies–Bouldin indices), and clustering stability (ARI). In addition, qualitative comparisons are performed through visualization in the t-SNE space to examine the similarity of cluster structures between stations.

Consistency between the clustering results of the two stations is interpreted as strong evidence that the detected clusters correspond to intrinsic operational states of the structure. Conversely, discrepancies between stations may indicate local effects, sensor noise, or potential anomalies in the monitoring system.

This multi-station validation strategy provides an additional layer of reliability beyond conventional single-station analysis. By incorporating spatial consistency as a validation criterion, the proposed framework enhances the robustness and practical applicability of unsupervised learning in structural health monitoring.

3. RESULTS AND DISCUSSION

3.1. Data quality and time segmentation

The quality of GNSS-RTK data plays a critical role in ensuring the reliability of subsequent analysis. In this study, statistical characteristics of the datasets collected from the two GNSS stations (4E and 4W) are first examined to assess data completeness and consistency.

A summary of the dataset is presented in Table 1. Both stations provide approximately 1.13 million observations over the monitoring period, corresponding to a sampling rate of 1 Hz for a duration of 14 days. As shown in Table 1, the datasets exhibit a high level of completeness, with 313 valid hours out of a total of 336 hours at each station.

Table 1. Summary of GNSS dataset.

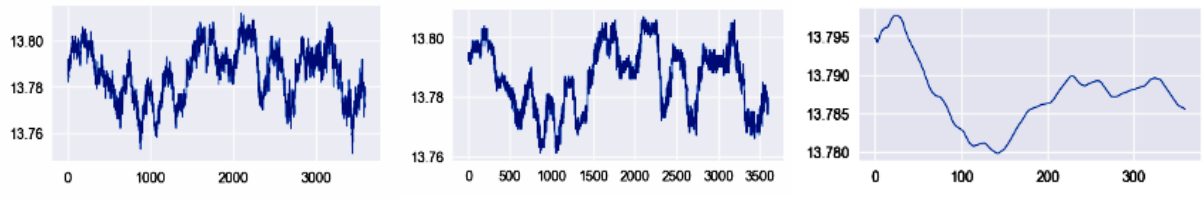
Parameter	Station 4E	Station 4W
Number of samples	~1,130,160	~1,130,256
Duration	14 days	14 days
Sampling rate	1 Hz	1 Hz
Total hours	336	336
Valid hours (no missing data)	313	313
Valid synchronized hours	238	238

To ensure robustness in the analysis, the continuous time series are segmented into hourly windows, each consisting of 3600 samples. Following the preprocessing criteria described in Section 2.2.1, time windows with more than 5% missing data are excluded. Furthermore, to maintain consistency in multi-station analysis, only time windows that are simultaneously valid at both stations are retained.

As a result, 238 synchronized time windows are selected for subsequent analysis. This synchronized dataset ensures that both stations are analyzed under identical operational and environmental conditions, thereby enabling a reliable assessment of spatial consistency in the detected operational states. This high level of data availability ensures the statistical reliability of subsequent clustering analysis.

3.2. Impact of preprocessing and dimensionality reduction

The effectiveness of the preprocessing steps is evaluated to assess their impact on improving data quality and enhancing the structure of the GNSS-RTK time series. The results of each preprocessing stage are illustrated in Figure 3.



(a) (b) (c)

Figure 3. Impact of preprocessing steps on GNSS time series: (a) raw data, (b) after outlier removal using the Hampel filter, and (c) after signal smoothing using the Kalman filter. The plots represent a representative segment of the time series.

The raw GNSS data (Figure 3a) exhibit significant noise and irregular fluctuations, including abrupt spikes caused by multipath effects and measurement errors. These outliers can distort the underlying signal and negatively affect the performance of clustering algorithms. After applying the Hampel filter (Figure 3b), most of the impulsive outliers are effectively removed. The resulting time series shows a clear reduction in extreme values while preserving the overall trend of the signal. This step is particularly important for GNSS data, where sporadic measurement errors are common. Subsequently, the Kalman filter is applied to further smooth the signal (Figure 3c). Compared to the Hampel-filtered data, the Kalman-filtered time series exhibits reduced random noise and improved continuity, allowing the main dynamic patterns of the structure to be more clearly observed.

Following preprocessing, the data are standardized and reduced in dimensionality using PCA. The results show that the first 50 principal components retain nearly all the variance of the original data (explained variance $\approx$ 100%), indicating that the essential information is well preserved despite the dimensionality reduction. This transformation also reduces redundancy and correlation among features, leading to a more compact and structured representation of the data.

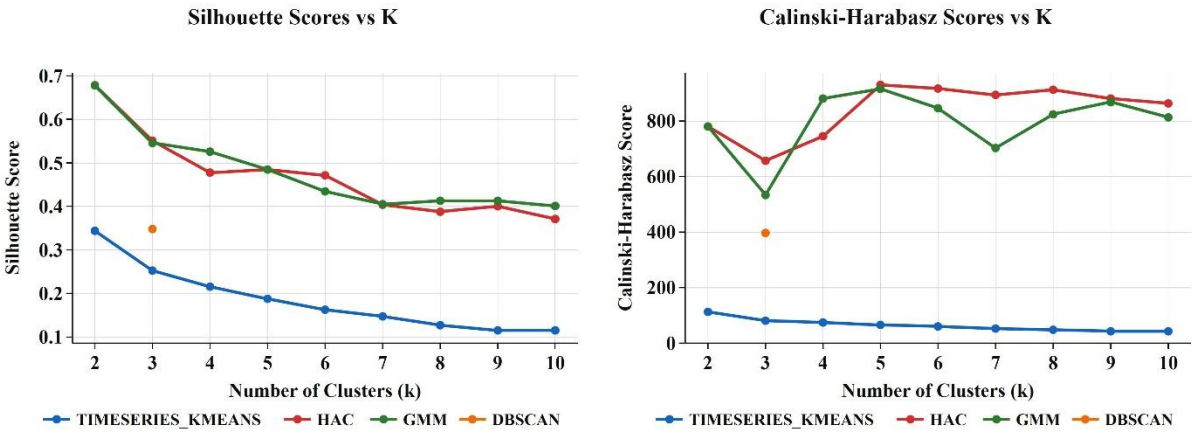
In addition, the t-SNE visualization (not used for clustering) reveals the emergence of distinguishable group patterns in the embedded space, suggesting the presence of latent cluster structures in the GNSS-RTK data.

Overall, the combination of Hampel filtering, Kalman smoothing, and PCA significantly improves data quality and enhances the separability of the feature space. These preprocessing steps provide a solid foundation for the clustering analysis presented in the following sections.

3.3. Determination of optimal number of clusters (k)

The determination of the optimal number of clusters is a critical step in clustering analysis, as it directly affects the interpretation of structural operational states. In this study, the optimal value of k is identified using a combination of internal validation metrics and a voting-based strategy, as described in Section 2.2.5.

For clustering algorithms that require a predefined number of clusters (K-Means, HAC, and GMM), the value of k is varied from 2 to 10. The Silhouette Coefficient is adopted as the primary evaluation criterion. As illustrated in Figure 4, the Silhouette score consistently reaches its maximum at $k = 2$ for both GNSS stations and across most clustering algorithms. When k increases beyond this value, the clustering quality gradually decreases, indicating reduced compactness and separation of clusters.



(a) (b)

Figure 4. Variation of clustering evaluation metrics with respect to the number of clusters k: (a) Silhouette coefficient and (b) Calinski-Harabasz index.

To further enhance the robustness of cluster selection, a voting-based approach is applied by aggregating the candidate values of k obtained from different algorithms and coordinate components. The results of this voting procedure are summarized in Table 2.

Table 2. Voting-based selection of the optimal number of clusters.

Component	Station 4E (Voting results)	Station 4W (Voting results)	Selected k (4E)	Selected k (4W)	Final k
X	K-Means (2), HAC (2), GMM (2)	K-Means (2), HAC (2), GMM (2)	2	2	2
Y	K-Means (2), HAC (2), GMM (2)	K-Means (2), HAC (2), GMM (2)	2	2	2
h	K-Means (2), HAC (2), GMM (2)	K-Means (6), HAC (5), GMM (2)	2	6	2

As shown in Table 2, the horizontal components (X and Y) exhibit strong consistency across both stations, with all algorithms selecting $k = 2$ as the optimal number of clusters. In contrast, the vertical component (h) shows some variability, particularly at station 4W, where different algorithms suggest larger values of k. This discrepancy is likely due to the higher noise level and lower signal quality in the vertical displacement measurements.

Although the vertical displacement component is physically important for characterizing bridge behavior at the mid-span, the clustering results indicate that operational states are less clearly separable in the h-component than in the longitudinal component. This finding suggests that additional preprocessing strategies may be required to improve the clustering performance of vertical GNSS displacement data.

Despite these local inconsistencies, the overall voting results clearly indicate that $k = 2$ is the most representative and stable choice. The agreement across multiple algorithms and between the two GNSS stations suggests that the two-cluster structure is an intrinsic characteristic of the GNSS-RTK data rather than an artifact of a specific method or measurement location.

This finding provides strong evidence that the structural response of the bridge can be effectively characterized by two dominant operational states under real-world conditions. Furthermore, the observed inconsistency in the vertical component supports the decision to focus on the horizontal displacement (X), which exhibits more stable and physically meaningful clustering behavior.

3.4. Clustering results

The clustering results obtained from different algorithms are analyzed to evaluate their effectiveness in identifying operational states from GNSS-RTK data. The results are visualized in the t-SNE space, as shown in Figure 5, while quantitative comparisons are summarized in Table 3.

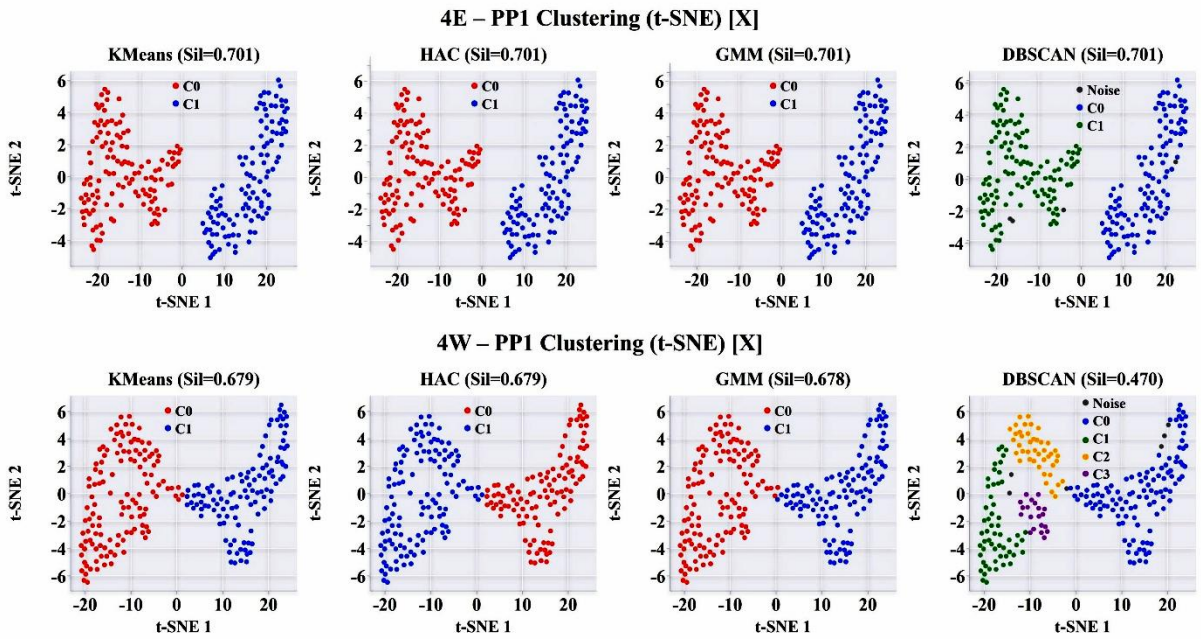


Figure 5. Clustering results in the t-SNE space for the two GNSS stations (4E and 4W), showing clear separation into two clusters for K-Means, HAC, and GMM, while DBSCAN exhibits a tendency toward cluster fragmentation.

Table 3. Comparison of clustering performance across algorithms on GNSS datasets (4E, 4W, and combined data) based on internal evaluation metrics.

Dataset	Algorithm	k	Silhouette	Calinski–Harabasz	Davies–Bouldin
4E	K-Means	2	0.7006	1102.9	0.4147
4E	HAC	2	0.7006	1102.9	0.4147
4E	GMM	2	0.7006	1102.9	0.4147
4E	DBSCAN	2	0.7006	1082.6	0.4150
4W	K-Means	2	0.6787	981.8	0.4461
4W	HAC	2	0.6787	981.8	0.4461
4W	GMM	2	0.6779	976.6	0.4481
4W	DBSCAN	4	0.4700	455.6	0.7936
4E+4W	K-Means	2	0.6529	1699.2	0.4851
4E+4W	HAC	2	0.6257	1483.6	0.5052
4E+4W	GMM	2	0.6529	1699.2	0.4851
4E+4W	DBSCAN	11	0.3988	1340.9	0.7221

For both GNSS stations (4E and 4W), the clustering results reveal a clear separation into two distinct groups when using K-Means, HAC, and GMM. The clusters exhibit well-defined boundaries with minimal overlap, indicating that the underlying structure of the data is effectively captured by these algorithms.

Among the tested methods, K-Means achieves the best performance, with the highest Silhouette scores of 0.7006 at station 4E and 0.6787 at station 4W. These results indicate strong intra-cluster cohesion and inter-cluster separation. HAC and GMM produce comparable results, suggesting that the clustering structure is robust and not highly sensitive to the choice of algorithm within this group.

In contrast, DBSCAN demonstrates lower performance and reduced stability. In particular, at station 4W, DBSCAN tends to fragment the data into multiple small clusters and exhibits lower clustering stability than the other methods. This behavior reflects the sensitivity of density-based methods to local variations in data density. At station 4W, the displacement observations appear to contain more heterogeneous density patterns than those observed at station 4E, leading DBSCAN to partition the data into several smaller clusters. However, additional analyses would be required to determine whether this effect is primarily caused by measurement noise or by intrinsic variations in structural response.

The consistent performance of distance-based and model-based algorithms (K-Means, HAC, and GMM) indicates that the data exhibit relatively compact and well-separated cluster structures. This finding suggests that the operational states of the bridge can be effectively represented by two dominant regimes.

Overall, the clustering results confirm that unsupervised learning methods can successfully identify consistent and reproducible patterns in GNSS-RTK data. The superior performance and stability of K-Means make it the most suitable method for the subsequent analysis.

Although the clustering framework successfully identified two distinct operational states, the present study does not attempt to assign a unique physical interpretation to each state because synchronized traffic, meteorological, and environmental measurements were not

available. Potential factors may include variations in traffic loading, environmental conditions, and temperature effects. However, the available dataset does not allow these influences to be evaluated separately. Nevertheless, the existence of two stable and reproducible clusters across both monitoring stations suggests that the detected states reflect distinct structural response regimes under varying operational and environmental conditions. Future studies integrating GNSS measurements with traffic and environmental data may provide a more comprehensive physical interpretation of the identified operational states.

In addition, the present study is based on a 14-day monitoring period under relatively normal operating conditions. Seasonal variations and extreme weather events, such as strong winds, heavy rainfall, or typhoons, may alter the structural response characteristics and potentially influence clustering behavior. Therefore, future research should investigate the robustness and transferability of the proposed framework using long-term monitoring data collected under diverse environmental conditions.

3.5. Comparison between GNSS stations

A key objective of this study is to evaluate the spatial consistency of the detected operational states across multiple GNSS monitoring stations. To this end, the clustering results obtained from stations 4E and 4W are systematically compared in both quantitative and qualitative aspects.

As shown in Table 3, the clustering performance metrics for the two stations are highly consistent. The Silhouette scores obtained by K-Means are 0.7006 for station 4E and 0.6787 for station 4W, indicating comparable levels of cluster cohesion and separation. Similarly, the Calinski–Harabasz and Davies–Bouldin indices exhibit close values between the two stations, further confirming the similarity in clustering quality.

In addition to quantitative agreement, the visual comparison in the t-SNE space (Figure 6) reveals that the cluster structures from both stations exhibit similar shapes, distributions, and separation patterns. The clusters are well aligned in terms of their relative positions and densities, suggesting that both stations capture consistent structural behavior.

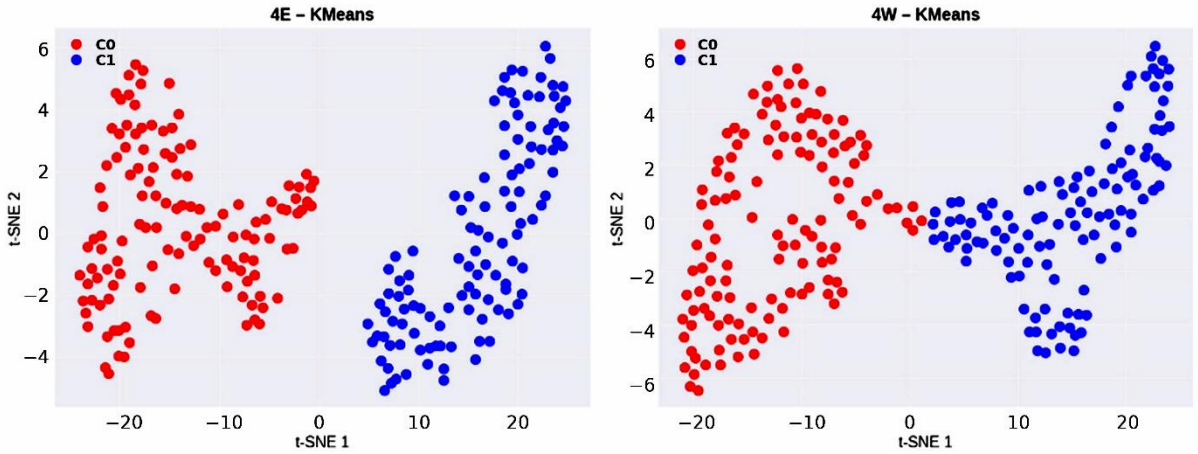


Figure 6. Comparison of clustering structures between the two GNSS stations (4E and 4W) in the t-SNE space using K-Means, showing a high degree of similarity in cluster shape, position, and size.

This consistency is particularly significant given that the two GNSS stations are located at different positions on the bridge. The observed agreement indicates that the identified clusters represent intrinsic operational states of the structure rather than artifacts caused by local measurement noise or sensor-specific effects.

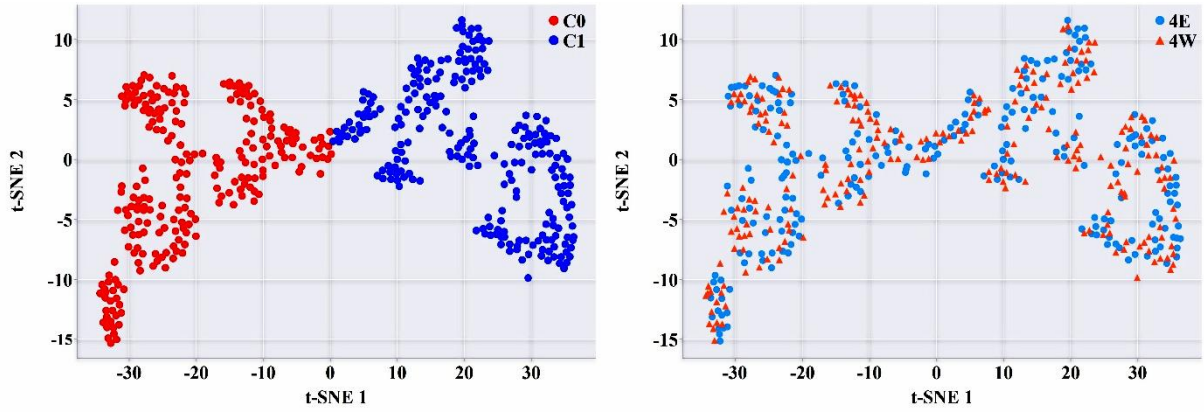
Furthermore, the convergence of results across stations provides strong validation for the robustness of the proposed framework. The ability to detect consistent clustering patterns from independent data sources enhances the reliability and practical applicability of the method for real-world structural health monitoring.

Overall, the high level of spatial consistency between stations 4E and 4W confirms that the detected two-cluster structure reflects genuine structural dynamics and can be interpreted as distinct operational states of the cable-stayed bridge.

3.6. Combined dataset analysis

To further evaluate the global consistency of the detected operational states, the datasets from the two GNSS stations (4E and 4W) are combined and analyzed jointly. This analysis aims to examine whether the clustering structure remains stable when data from multiple monitoring locations are integrated.

The clustering results for the combined dataset are presented in Figure 7. As shown in Figure 7a, the data are still clearly separated into two distinct clusters in the t-SNE space, indicating that the two-cluster structure is preserved even after merging the datasets.



(a) (b)

Figure 7. Clustering results for the combined dataset from two GNSS stations (4E and 4W) using K-Means in the t-SNE space: (a) clustering results (C0, C1); (b) distribution of data points by station (4E and 4W).

More importantly, Figure 7b shows that data points from both stations are intermingled within the same clusters rather than forming separate groups based on station identity. This observation suggests that the clustering results are not influenced by the measurement location, but instead reflect common structural behavior shared across the bridge.

Quantitative results in Table 3 further support this observation. K-Means maintains strong performance on the combined dataset, achieving a Silhouette score of 0.6529, while GMM produces comparable results. In contrast, DBSCAN shows significantly lower performance (Silhouette score ≈ 0.3988), indicating reduced effectiveness in handling data with varying density distributions.

The consistency of clustering performance across individual and combined datasets confirms that the detected clusters are robust and not dependent on specific monitoring locations. This reinforces the interpretation that the two clusters correspond to intrinsic operational states of the structure.

Overall, the combined dataset analysis provides strong evidence that the proposed framework can generalize across multiple monitoring points and capture global structural behavior. This capability is essential for practical applications of structural health monitoring systems, where data from multiple sensors must be integrated and interpreted in a unified manner.

3.7. Clustering stability analysis

The stability of clustering algorithms is evaluated using the ARI, which measures the consistency of clustering results across multiple runs with different initializations. The results are summarized in Table 4.

Table 4. Stability of clustering algorithms based on ARI (mean ± standard deviation).

Algorithm	Station 4E	Station 4W
K-Means	1.000 ± 0.000	1.000 ± 0.000
HAC	1.000 ± 0.000	0.467 ± 0.469
GMM	1.000 ± 0.000	1.000 ± 0.000
DBSCAN	0.616 ± 0.242	0.739 ± 0.187

Note: ARI = 1 indicates perfectly stable clustering results across runs.

The results show that K-Means and GMM achieve perfect stability at both stations, with ARI values equal to 1.000 and zero standard deviation. This indicates that the clustering results are fully consistent and independent of initialization conditions. In contrast, HAC exhibits a significant decrease in stability at station 4W, with a mean ARI of 0.467 and a large standard deviation. This behavior suggests that hierarchical clustering is sensitive to noise and linkage structures, particularly in high-dimensional feature spaces. DBSCAN demonstrates moderate stability, with ARI values ranging from 0.616 to 0.739. This reflects its sensitivity to parameter selection and variations in data density, which are common characteristics of GNSS-RTK data.

These findings are particularly important in structural health monitoring applications, where reliable and stable results are essential for long-term monitoring. Overall, the results highlight the importance of selecting algorithms that ensure both high clustering quality and stability, with K-Means emerging as the most robust method in this study.

4. CONCLUSION

This study proposes an UL framework for detecting operational states of cable-stayed bridges using multi-station GNSS-RTK data. The results reveal a clear and stable two-cluster structure in the horizontal displacement component. Among the evaluated methods, K-Means achieves the best performance, with high clustering quality (Silhouette up to 0.7006) and perfect stability (ARI = 1.000).

The consistency of clustering results across two independent GNSS stations, as well as in the combined dataset, confirms that the detected clusters represent intrinsic structural behavior rather than sensor-specific effects. These findings demonstrate that unsupervised learning provides a reliable and scalable approach for structural health monitoring using GNSS-RTK data. Future work will focus on improving the analysis of the vertical displacement component, which is physically important for mid-span bridge monitoring, through advanced denoising, sensor-fusion approaches, temporal modeling, and more sophisticated learning techniques.

REFERENCES

[1]. G. W. Roberts, X. Meng, A. H. Dodson, Integrating a global positioning system and accelerometers to monitor the deflection of bridges, Journal of Surveying Engineering, 130 (2004) 65–72. https://doi.org/10.1061/(ASCE)0733-9453(2004)130:2(65)

[2]. K. G. Le, D. C. Tran, T. L. H. Ho, Self-supervised deep learning for GNSS time series imputation: A comparative study of neural network architectures, Transport and Communications Science Journal, 77 (2026) 127–141. https://doi.org/10.47869/tcsj.77.1.10

[3]. P. J. G. Teunissen, O. Montenbruck, Springer Handbook of Global Navigation Satellite Systems, Springer International Publishing, Cham, 2017.

[4]. K. Worden, C. R. Farrar, G. Manson, G. Park, The fundamental axioms of structural health monitoring, in: Proceedings of the Royal Society A, 463 (2082) (2007) 1639–1664. https://doi.org/10.1098/rspa.2007.1834

[5]. T. L. H. Ho, D. C. Tran, V. V. Le, K. G. Le, Latent pattern recognition in GNSS-based SHM using t-SNE and adaptive time-series modeling, Journal of Civil Structural Health Monitoring, 15 (2025) 3743–3766. https://doi.org/10.1007/s13349-025-01014-9

[6]. D. C. Tran, T. L. H. Ho, K. G. Le, V. H. Le, Application of unsupervised clustering algorithms in GNSS-RTK data analysis for cable-stayed bridge monitoring, Transport and Communications Science Journal, 76 (2025) 1138-1150. https://doi.org/10.47869/tcsj.76.8.8 (in Vietnamese).

[7]. Ministry of Transport of Vietnam, Design and installation documentation of Nhat Tan Bridge monitoring system, 2015.

[8]. F. Pedregosa, G. Varoquaux, A. Gramfort, V. Michel, B. Thirion, O. Grisel, et al., Scikit-learn: Machine learning in Python, Journal of Machine Learning Research, 12 (2011) 2825–2830.

[9]. H. Abdi, L. J. Williams, Principal component analysis, Wiley Interdisciplinary Reviews: Computational Statistics, 2 (2010) 433–459. https://doi.org/10.1002/wics.101

[10]. L. van der Maaten, G. Hinton, Visualizing data using t-SNE, Journal of Machine Learning Research, 9 (2008).

[11]. A. Dudek, Silhouette index as clustering evaluation tool, in: Conference of the Section on Classification and Data Analysis of the Polish Statistical Association, Springer, (2019) 19–33. https://doi.org/10.1007/978-3-030-52348-0_2

[12]. D. A. Reynolds, Gaussian mixture models, Encyclopedia of Biometrics (2009) 659–663. https://doi.org/10.1007/978-0-387-73003-5_196

[13]. F.-M. Bi, W. Wei, C. Long, DBSCAN: Density-based spatial clustering of applications with noise, Journal of Nanjing University (Natural Sciences), 48 (2015) 491–498.

[14]. X. Wang, Y. Xu, An improved index for clustering validation based on Silhouette index and Calinski–Harabasz index, IOP Conference Series: Materials Science and Engineering, 569 (2019) 052024. https://doi.org/10.1088/1757-899X/569/5/052024

[15]. M. Mughnyanti, S. Efendi, M. Zarlis, Analysis of determining centroid clustering X-means algorithm with Davies–Bouldin index evaluation, IOP Conference Series: Materials Science and Engineering, 725 (2020) 012128. https://doi.org/10.1088/1757-899X/725/1/012128

[16]. L. Hubert, P. Arabie, Comparing partitions, Journal of Classification, 2 (1985) 193–218. https://doi.org/10.1007/BF01908075